Study on Wear Resistance of Al-Si Alloy using A 3-Body Dry Abrasive Wear Testing Machine

Manjot Singh Saini
Metallurgical and Materials Engineering Department,
MSU, Vadodara, Gujarat, India

Monil Salot
Department of Metallurgical and Materials Engineering
IITE, Indus University,
Ahmedabad, India

Samanvay Shah
Department of Metallurgical and Materials Engineering
IITE, Indus University,
Ahmedabad, India

Mandar Joshi,
LE College, Morbi, Gujarat,
India

***Abstract*—Material loss due to wear may result in catastrophic failure in wide variety of application. Since wear is a progressive process and gives prior warning before the failure, it is possible to overcome wear related failure by taking proper corrective actions. The gradual removal of a material(s) from one or both surfaces in contact during motion increases the clearance between the surfaces. This spatial freedom induces vibration that often leads to fatigue failures of machinery components. Wear of material takes place via different mechanisms. Abrasive wear is one such mechanism where the material from a relatively softer surface is ploughed away by hard particles either during sliding or rolling motion. The particles may be loose debris from parent material or foreign material. This study focuses on the evaluation of abrasive wear resistance of Al-Si alloys with and without chromium oxide coating. The abrasive wear testing was performed as per ASTM G-65 using dry sand and rubber wheel. The amount of Si in Al alloys was varied to 5%, 10%, and 14% and their relative wear performance was evaluated. As expected, it is observed that the wear resistance of Al-Si alloys increases with the increase in the amount of Si in the alloy. The hardness of Chromium oxide coating was greater than the base alloy; however, the wear resistance of chromium oxide coated samples was inferior vis-à-vis uncoated samples. This is due to the weak interfacial bonding between the coating and base material.**

Keywords — Wear; abrasive wear; ASTM G-65; Al-Si alloys; chromium oxide coatings

1. INTRODUCTION

Wear is a phenomenon observed at surfaces and can be defined as a progressive loss of material subjected to load and relative motion. Wear is related to interactions between surfaces and more specifically the removal and deformation of material on a surface as a result of mechanical action of opposite surface. In any mechanical equipment, the relative motion either in the form of sliding, rotating, reciprocating, impact, etc. results in loss of material due to wear. There are five modes of wear. These are: abrasive, adhesive, fretting, corrosive and fatigue wear. [5-10]

Abrasive wear occurs when hard materials, metals, sand, grit and dust move along the surface under load indenting the surface. It takes place when hard asperities or third phase particles rub under load on a relatively softer surface. Various abrasive wear mechanisms are plowing, wedging and cutting. The Figure 1 depicts some of the processes which are possible when a single abrasive tip slides across a surface. They include plowing, wedge formation, cutting, microfatigue, and microcracking.

The two modes of abrasive wear are two-body and three-body abrasive wear. In two-body abrasion, wear is caused by hard protuberances on one surface which can only slide over the other; whereas in three-body abrasion, particles are trapped between two solid surfaces but are free to roll and slide. The schematic diagram illustrating the mechanism of 2-body abrasive wear and 3-body abrasive wear is shown in Figure 2. The rate of material removal in 3-body abrasion is one order of magnitude lower than that for 2-body abrasion. This is because the loose abrasive particles abrade the solid surfaces for only about 10% of the time during sliding, while they spend about 90% of time in rolling. Most of the abrasive wear problems, which arise in agricultural and industrial equipment, are 3-body, while 2-body abrasion is encountered primarily in material removal operations.

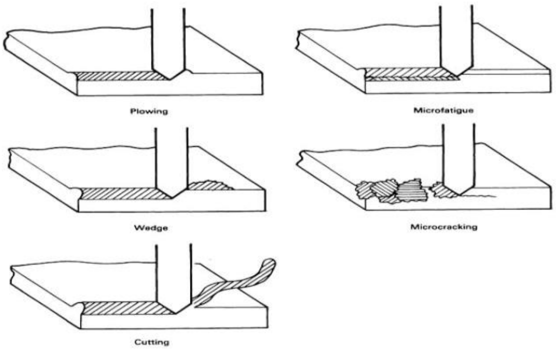

Figure 1: Mechanism of abrasive wear.

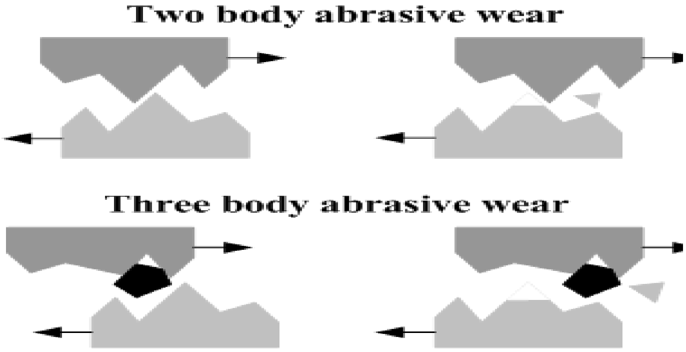

Figure 2: Two-body and Three-body abrasive wear.

A 3-body dry abrasive wear testing machine is based on the principle of rolling and sliding of particles down a moving surface. The testing machine is based on parameters described by ASTM G-65 for dry sand rubber wheel test. [14]

Aluminium alloys are designated according to their major alloying elements. The 3xx group contains silicon as the primary alloying element. This is because it increases the fluidity of the melt, reduces the melting temperature, decreases the shrinkage during solidification and is relatively inexpensive. [1-3]

Silicon also has a low density (2.34 g cm^{-3}), which may be an advantage in reducing the total weight of the cast component. Silicon has a very low solubility in aluminium; it therefore nucleates and grows as eutectic phase.

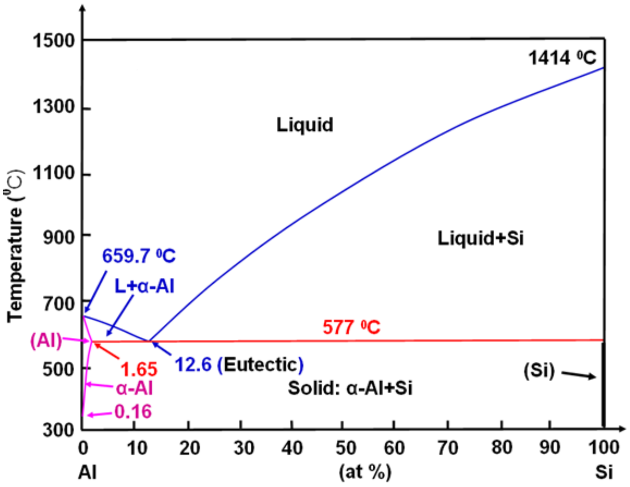

Figure 3: Phase diagram Al-Si Alloy. [4]

In this study, wear performance of Al-Si alloys are evaluated. Al-Si alloys have excellent castability and are widely used in automotive industries. The presence of Si in Al alloys increases its castability but also offers reasonable wear resistance. In hypoeutectic Al-Si alloys, Si is distributed as eutectic phase in interdendritic regions; whereas in hypereutectic Al-Si alloys, Si exists both as primary and eutectic phases. [11-12] In general, the abrasive wear resistance of Al-Si alloy increases with the increase in Si content. This is because Si is hard phase and it offers resistance to abrasion. However, in many challenging applications, the abrasive wear resistance of Al-Si alloys (irrespective of its composition) is inadequate. Therefore, it is imperative to engineer the surface of components made from Al-Si alloy and enhance their abrasive wear resistance. The objective of surface engineering is to upgrade their functional capabilities keeping the economic factors in mind. [15]

There are various ways to produce relatively hard coating on Al-Si alloys. Thermal spraying technique [13] is one of the potentially attractive methods to coat Al-Si alloys with hard material. In this method, molten materials are sprayed on the substrate. The "feedstock" (coating precursor) is heated by electrical (plasma or arc) or chemical means (combustion flame). The process has been successfully used to provide thick coatings (approx. thickness range is 20 micrometres to several mm, depending on the process and feedstock) over a large area at high deposition rate.

2. EXPERIMENTAL PROCEDURE

2.1 Specimen preparation

Al–Si alloys with varying Si percentage were prepared by melting commercially pure aluminium (99.7%) and master alloy of Al-14%Si in a graphite crucible in a high frequency induction furnace. The melt was held at 800°C in order to attain homogeneous composition. The melt was poured into cast iron mold to prepare samples with following dimensions: 73mm x 48mm x 9mm. The chemical composition of the cast alloys was determined using optical emission spectrometer. Castings following compositions were prepared: Al- 5% Si, Al- 10%Si and Al- 14%Si. Cylindrical samples of 20 mm diameter and 10 mm height were machined from the casting for 3-body abrasion testing.

2.2 Optical microscopy

Microstructures of samples were observed under computerized optical microscope. The metallographic samples of Al-Si alloys with varying amount of Si were prepared by grinding and polishing using various grits of emery paper as per ASTM E3 standard specification. Each sample was etched using aluminium salfita reagent. The main constituents of this reagent are water (190ml), hydrofluoric acid (2ml), hydrochloric acid (3ml).

2.3 Chromium oxide coating

The chromium oxide coating (Cr_2O_3) was deposited on Al-Si alloys to enhance their wear resistance. Prior to the deposition of Cr_2O_3, the surface of the sample was cleaned by shot blasting process, followed by a pre-coat of Nickel-Aluminium. The pre-coat of Ni-Al alloy is required to provide adequate bonding strength between Cr_2O_3 and the substrate. The Cr_2O_3 material was deposited on Al-Si alloys by thermal spraying – High velocity oxygen fuel (HVOF) coating process. During HVOF process, chromium oxide powder is melted using combustion flame at the tip of the nozzle. The combustion flame was generated from mixture of oxygen (4 bar pressure) and acetylene fuel (7.5 bar pressure). The flame tip can reach temperature ranging from 3000-3500 °C. The thermal flame is directed onto samples to coat it with Cr_2O_3 coating. The Cr_2O_3 droplets in mushy is deposited on the substrate. The pressure used for coating process is 4 bar. The schematic diagram of HVOF coating process is shown in

Figure 4. Thermal spray HVOF coating of Cr_2O_3 on Al-Si alloys was performed at Keepsake Engineering Consultancy, Ahmedabad, India. Properties of chromium oxide coating were evaluated by hardness measurement and wear testing.

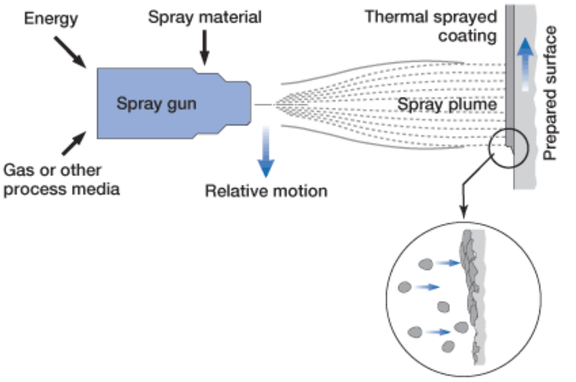

Figure 4: Thermal spraying coating process.

2.4 *Brinell hardness testing*

Brinell hardness measurements were performed on various Al-Si alloys with and without coating. The Brinell hardness number (BHN) is calculated using the equation:

$$BHN = 2F/\pi D(D-(D^2-D_i^2)^{1/2})$$

Where: F is the applied load, and D is the diameter of indent.

2.5 *Wear test*

Three body dry abrasive wear testing was performed on various Al-Si alloys (both with and without coating). The wear testing was performed as per ASTM G-65 standard. The 3-body wear tester is shown in Figure 5. The abrasive wear test consists of following steps: 1) Sample was held stationary in the holder, 2) Required normal load was applied through a lever mechanism, and 3) Abrasive particles (quartz sand, -36 mesh) was fed between the sample and the wheel rotating at a speed of 1300 rpm for 1 minute. The amount of volume loss was calculated by weight loss method. Care has been taken that the specimens under test are continuously cleaned with woolen cloth to avoid the entrapment of wear debris to get the uniform results.

Figure 5: 3-body abrasive wear testing machine

2.6 *Microscopy*

Optical Microscopy

Microstructural examination was performed on various Al-Si alloys by an optical microscope. Sample from each alloy was metallographically prepared as per ASTM E3 standard specification. The Al-Si sample was mechanically ground and polished using different grits of emery paper and final polishing was performed using Alumina powder of 0.1μm size. Prior to microstructural examination, each sample was etched with Keller's reagent (1 volume part of hydrofluoric acid (48%), 1.5 volume part of hydrochloric acid, 2.5 volume parts of nitric acid and 95 volume parts of water).

Scanning electron microscopy (SEM)

Worn surface of various samples (with and without coating) was characterized using SEM to determine the wear mechanism.

3. RESULT AND DISCUSSION

3.1 *Microstructural analysis of as-cast samples*

Figure 6 (a) and (b) shows optical micrographs of Al-5% Si and Al-10% Si alloys. As expected, both of these alloys shows dendritic microstructure with interdendritic eutectic Si. The morphology of eutectic Si is flaky type, which is typical in unmodified hypoeutectic Al-Si alloys. In general, the volume fraction of eutectic Si in Al-10% Si is much greater than in Al-5% Si alloy. In contrast to hypoeutectic Al-Si alloy, the hypereutectic alloy (Al-14% Si) shows blocky primary Si and flaky eutectic Si (Figure 6(c)).

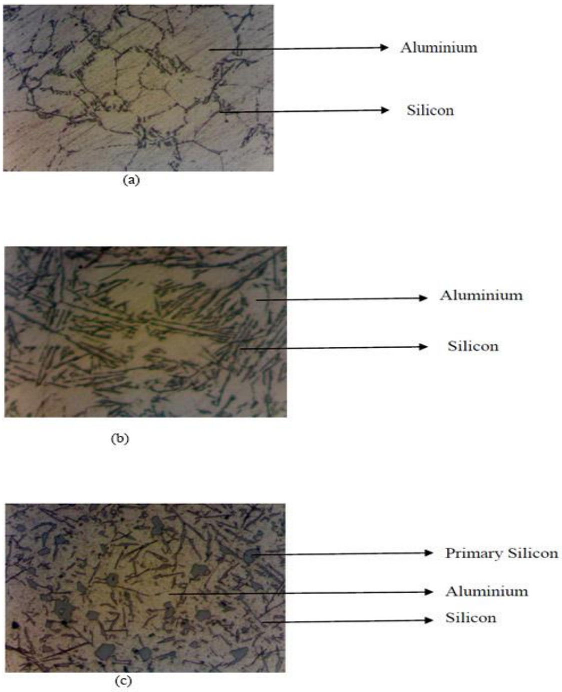

Figure 6: Microstructure of as-cast (a) Al-5% Si, (b) Al-10% Si, and (c) Al-15% Si alloys.

3.2 *Brinell hardness test*

For each sample, two hardness measurements were performed and average value is reported. Variation in hardness value with Si content of uncoated Al-Si alloy is shown in Figure 7. As expected, hardness of Al-Si alloy increases with the increase in Si content.

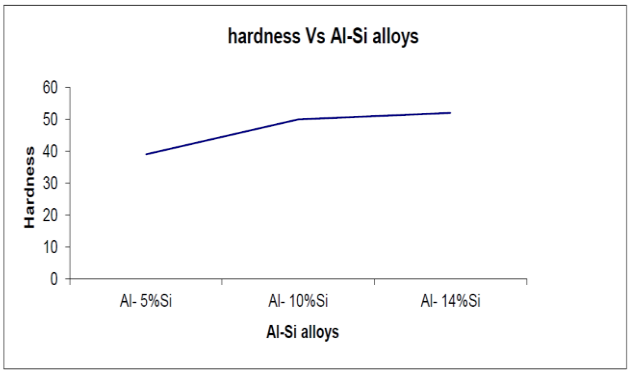

Figure 7: Hardness test for as-cast samples

Variation in hardness of Al-Si alloys coated with Cr_2O_3 is shown in Figure 8. In general, the hardness of coated Al-Si alloy is greater than the uncoated alloy. In addition, the hardness of coated alloy also depends on the thickness of the coating. In general, it shows marginal increase in hardness with the increase in coating thickness.

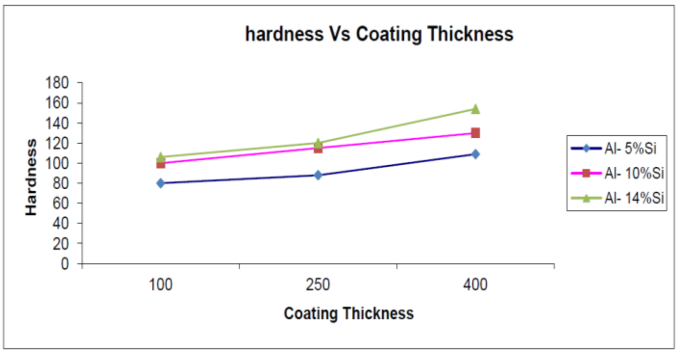

Figure 8: Hardness test for coated samples

3.3 *Wear test*

Wear Performance of uncoated Al-Si Alloys

The wear tests of Al-Si alloys were carried out using 3-body dry abrasive wear testing machine. Quartz sand (36 mesh) was used as abrasive media and was fed with flow rate of 350 g/min. The test load was kept constant at 20 N with wheel rotating at a speed of 1300rpm. Each sample was tested for 1 minute. Wear volume was calculated based on mass loss method. Wear test results of Al-Si alloy are shown in Table 1.

Table 1: Wear test results of as-cast samples.

Al- 5%Si							
S.no.	Volume(cm^3)	Initial mass	Density(g/cc) **(Initial mass/ Volume)**	Final mass	Mass loss	Volume Loss(mm^3) **(Mass loss/ Density)*1000**	Avg
1	31.536	108.76	3.449	108.48	0.28	81.183	
2	31.536	108.5	3.441	108.25	0.25	72.653	
3	31.536	108.91	3.454	108.64	0.27	78.17	77.335
Al- 10%Si							
S.no.	Volume(cm^3)	Initial mass	Density(g/cc) **(Initial mass/ Volume)**	Final mass	Mass loss	Volume Loss(mm^3) **(Mass loss/ Density)**	Avg
1	31.536	100.18	3.177	99.98	0.2	62.952	
2	31.536	98.21	2.803	98.01	0.2	71.352	
3	31.536	96.92	3.073	96.74	0.18	58.575	64.293
Al- 14%Si							
S.no.	Volume(cm^3)	Initial mass	Density(g/cc) **(Initial mass/ Volume)**	Final mass	Mass loss	Volume Loss(mm^3) **(Mass loss/ Density)**	Avg
1	31.536	110.1	3.491	109.99	0.11	31.51	
2	31.536	110.56	3.505	110.43	0.13	37.099	
3	31.536	110	3.488	109.9	0.1	28.67	32.423

It is observed that with increase of Si from 5% to 14 %, the wear volume loss decreases from 77.335 to 32.423 cm^3, respectively (Figure 9). This is consistent with hardness measurement where it is noted that the hardness of the Al-Si alloy increases with the increase in Si content.

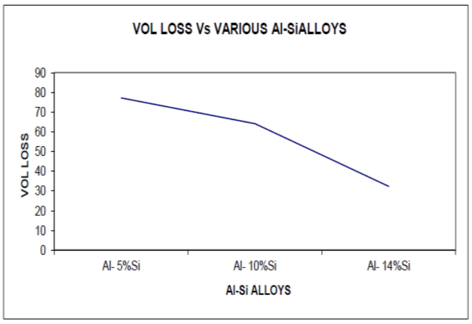

Figure 9: wear test result graph as-cast samples

Wear Performance of Al-Si Alloys coated with Cr_2O_3

Wear test results of Al-Si alloy are shown in Table 2. Variation in wear volume loss of various samples is shown in Figure 10. It is observed that irrespective of the amount of Si in the alloy, the wear volume loss of the sample decreases with increase in coating thickness from 100 µm to 400 µm. In general, the wear volume loss of the coated samples is greater than the uncoated samples. This is due to the lack of adequate bonding between the substrate and Cr_2O_3 coating.

Table 2: Wear test results of coated Al-Si samples.

Al- 5%Si (Coated with Cr_2O_3)							
S.no.	Coating thickness (μm)	Volume (cm^3)	Initial mass	Density(g/cc) **(Initial mass/ Volume)**	Final mass	Mass loss	Volume Loss(mm^3) **(Mass loss/ Density)* 1000**
1	100	16.243	45.54	2.76	44.9	0.64	234
2	250	16.243	47.55	2.89	46.96	0.59	205
3	400	16.243	48.67	2.96	48.17	0.5	170
Al- 10%Si (Coated with Cr_2O_3)							
S.no.	Coating thickness (μm)	Volume (cm^3)	Initial mass	Density(g/cc) **(Initial mass/ Volume)**	Final mass	Mass loss	Volume Loss(mm^3) **(Mass loss/ Density)**
1	100	16.243	42.97	2.76	42.52	0.45	174
2	250	16.243	45.33	2.89	44.91	0.42	153
3	400	16.243	43.32	2.96	43	0.32	121
Al- 14%Si (Coated with Cr_2O_3)							
S.no.	Coating thickness (μm)	Volume (cm^3)	Initial mass	Density(g/cc) **(Initial mass/ Volume)**	Final mass	Mass loss	Volume Loss(mm^3) **(Mass loss/ Density)**
1	100	16.243	48.31	2.94	47.89	0.42	143
2	250	16.243	51.86	3.16	51.44	0.42	134
3	400	16.243	52.69	3.22	52.46	0.23	71

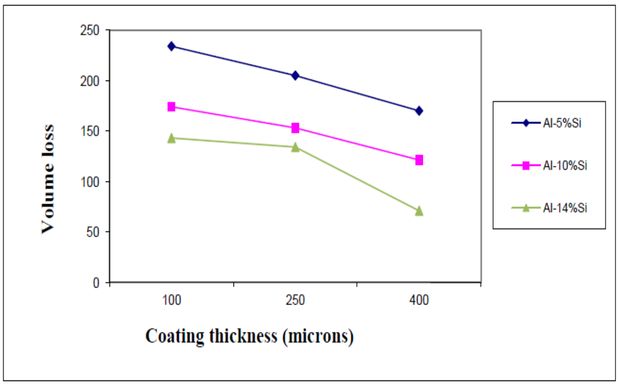

Figure 10: wear test result graph coated samples

3.4 *SEM Analysis*

The interface adhesion of the coatings depends on the coating morphology and interparticle bonding of the sprayed powders. SEM micrograph of the coatings of 100, 250 & 400 micron thickness are shown in Figures 11-14. Large volume of cavitations along with some large pores on the interparticle boundaries and triple particle junctions are observed on samples with coating of thickness = 100μm (Figure 11). This may have originated during solidification of particles from un/semi-molten state and consequently resulted in less adhesion of coating with the substrate. On contrary, the coating of thickness = 250μm (Figure 12), shows different worn morphology. Large number of globular particles and some flattened regions (an indicative of solidification of molten species during spray deposition) are observed. Amount of cavitations in thicker coating (i.e. 250 μm thick) is less than that in coating relatively thin coating (i.e. 100 μm). Coating of thickness = 400μm (Figure 13) shows uniform distribution of molten/semi molten particles. Larger portions of the coating exhibit flattened region, which might have been formed during solidification of molten species that have fused together in lumps. Less cavitation is observed at grain boundaries.

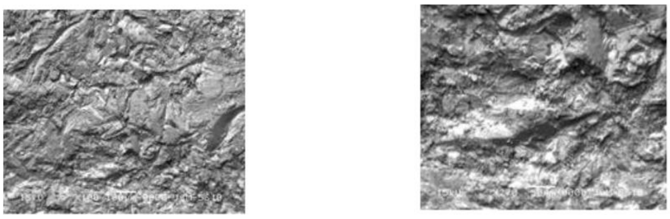
(a) (b)

Figure 11: SEM images of worn surface of Al- 10%Si with 100 micron coating at (a) 50X and (b) 100X

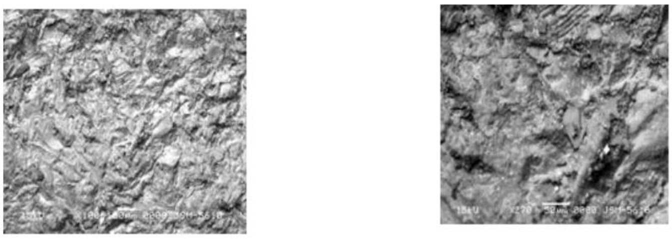
(a) (b)

Figure 12: SEM images of worn surface of Al- 10%Si with 250 micron coating at (a) 50X and (b) 100X


(a) (b)

Figure 13: SEM images of worn surface of Al- 10%Si with 400 micron coating at (a) 50X and (b) 100X


(a) (b)

Figure 14: SEM images of worn surface of Al- 10%Si without coating at (a) 50X and (b) 100X

4. CONCLUSIONS

Following conclusions are drawn from this investigation:

1. Microstructural examination shows that the volume fraction of silicon increases with increase in percentage of silicon from 5% to 14% in Al-Si alloy.
2. Hardness of the as-cast and chromium oxide coated samples increases with the increase in amount of silicon.

3. It is observed that hardness of the coated samples increases with increase in thickness of coating.
4. The hardness of uncoated samples is significantly lower than the coated samples.
5. The wear volume loss of Al-Si alloy decreases with increase in silicon percentage.
6. The wear volume loss of the coated sample is less uncoated samples. This is attributed to the poor quality of coating on the samples. Further optimization of thermal spray coating is required to produce coating of superior quality.

5. REFERENCES

[1] Elwin L. Rooy "Introduction to Aluminum and Aluminum Alloys" ASM Handbook Vol-02
[2] Singh Vijendra, “Physical Metallurgy”, Delhi, Standard Publishers Distributors, 2008
[3] Hatch John E, “Aluminium: Properties and Physical Metallurgy”, ASM, 1984, Metals Park, Ohio
[4] Murray J.L., McAlister A.J.; ASM Handbook Volume 3: Alloy Phase Diagrams, pp. 312
[5] Tylczak Joseph H., Oregon Albany, “Abrasive Wear”, Wear, ASM handbook, vol-18
[6] Kosel Thomas H, “Solid Particle Erosion”, Wear, ASM handbook, vol-18
[7] Ludema K C, “Sliding and Adhesive wear”, Wear, ASM handbook, vol-18
[8] Waterhouse R.B, "fretting wear", wear, ASM handbook vol-18
[9] Madse Brent W, "Corrosive Wear", Wear, ASM handbook, vol-18
[10] Engel Peter, "Impact Wear", wear, ASM handbook, vol-18
[11] Davis J. R., Aluminum and aluminum alloys, J. R. Davis & Associates, ASMInternational. Handbook Committee, pp 3-8.
[12] Torabian H., Pathak J.P. and Tiwai S.N.; Wear Characteristics of Al-Si alloys, Wear, Vol. 172 (1994), pp. 49-58.
[13] Thermal Spray Coatings Burton A. Kushner and Edward R. Novinski, Perkin-Elmer Corporation, Metco Division asm handbook vol. 18.
[14] ASTM G-65 Standard Test Method for measuring Abrasion Using the Dry Sand/Rubber Wheel Apparatus.
[15] Cornell R., Bhadeshia H.K.D.H; Aluminium-Silicon Casting Alloys